prosthesis

MDPI

Case Report

Ascending Aorta Resection and End-to-End Anastomosis: Redistribution of Wall Shear Stress Induced by a Bioprosthetic Heart Valve

Giuseppe M. Raffa [1] and Salvatore Pasta [2,*]

[1] Mediterranean Institute for Transplantation and Advanced Specialized Therapies (ISMETT), Via Tricomi n.5, 90100 Palermo, Italy; graffa@ismett.edu
[2] Department of Engineering, University of Palermo, Viale delle Scienze Ed.8, 90128 Palermo, Italy
* Correspondence: salvatore.pasta@unipa.it; Tel.: +39-3349379694

Received: 4 September 2020; Accepted: 29 September 2020; Published: 9 October 2020

Abstract: Although aortic resection and end-to-end anastomosis are applied to repair ascending aortic aneurysm, there is a lack of information on the late risk of post-operative complications, such as aortic dissection and aneurysmal re-dilatation. It is recognized that altered hemodynamic forces exerted on an aortic wall play an important role on dissection and aneurysm formation. We present a case in which the hemodynamic forces were investigated prior and after repair of an ascending aorta treated by resection with end-to-end anastomosis and a bioprosthetic heart valve. Post-operative wall shear stress was redistributed uniformly along the vessel circumference, and this may suggest a reduced risk of complications near aortic root, but not exclude the re-dilatation of the ascending aorta.

Keywords: aorta/aortic; aortic dissection; aneurysm; ascending aorta; computational fluid dynamic

1. Introduction

Aortic resection and end-to-end anastomosis have been proposed to treat ascending aortic aneurysms [1]. Changes in hemodynamic parameters within the aortic lumen and after aortic resection have not been investigated yet. There are indeed inconsistencies in the surgical practice with regards to the extent of the surgical aortic resection, while the risk of late re-dilatation after aortoplasty is remarkable in patients with an extended aneurysm. In this context, the reduction and redistribution of shear forces may prevent the risk of further aortic dilatation, dissection, and rupture. Computational fluid dynamic analysis can be used to estimate the redistribution of wall shear stress (WSS) on the repaired aortic wall, and thus improve the rationale of the surgical procedure by developing patient-tailored approaches [2,3]. Indeed, there is a need for additional information regarding the risk of re-dilatation of the aneurysmal ascending aorta, so that patient-specific computational flow analysis may reveal insights in the post-operative hemodynamic scenario induced by the surgical remodeling of the ascending aorta. This can lead to the identification of patients at high risk of re-dilatation of the aorta and ultimately improve the rationale of the surgical procedure by developing patient-tailored approaches.

We here present a study where computational modeling was used to demonstrate changes in the hemodynamics, as dictated by the bioprosthetic valve leaflets after aortic resection.

2. Materials and Methods

2.1. Case Study

A 63-year-old man was diagnosed with severe aortic valve regurgitation conditioning mild left ventricular enlargement (LV end diastolic volume 170 mL, LVEF 55%) and functional limitation

(NYHA III). A preoperative cardiac CT confirmed an aortic dilatation of 46 mm and tricuspid aortic valve. He underwent aortic valve replacement with a bioprosthetic heart valve (22 mm Perimount, Carpentier-Edwards) and ascending aortic resection with end-to-end anastomosis. With the pump on, the heart was decompressed, and the aorta was then completely mobilized from the surrounding structures. A short tract of the ascending aorta was resected between two circumferential aortotomies: the first at the level of the sino-tubular junction and the second at the distal edge of the dilatation. Then, the two ends of the aorta were finally sutured, and the aortic cross clamp was released. The post-operative course was uneventful, and the patient was discharged home after 7 days. After resection, the aortic diameter was 36.5 mm at CT scan. The angle between the longitudinal axis of the left ventricle and the aortic root was 148° before surgery and 156° after aortic resection. Figure 1 shows the pre- and post-operative CT scans of the patient.

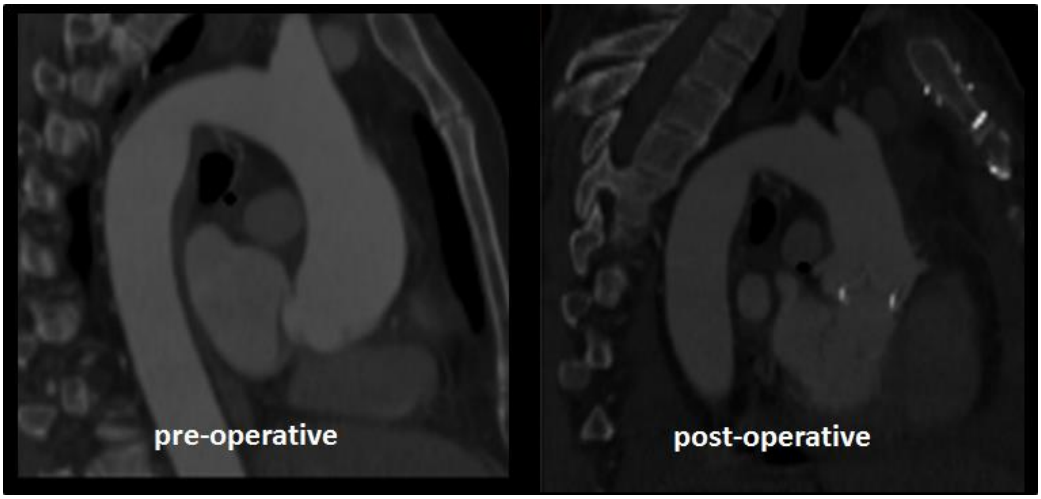

Figure 1. Pre- and post-operative CT images showing the change in the aortic shape induced by surgical remodeling.

2.2. Computational Flow Analysis

Pre- and post-operative aortic geometries were reconstructed from the patient's CT scans using the medical imaging software Mimics v20 (Materialise, Leuven, Belgium). Specifically, semi-automatic threshold-based segmentation permitted one to segment the aortic lumen, with the tricuspid aortic valve geometry reconstructed at fully opened shape [4]. The post-operative model had a circular shape for the inlet flow due to the bioprosthetic aortic valve replacement. Indeed, the bioprosthesis was not clearly visible at CT scans, so that we preferred to ideally represent the device with a circular shape with an orifice area of 4 cm^2. Once the aortic anatomy was reconstructed, the mesh was realized with ICEM software (Ansys Inc., Canonsburg, PA, USA) using unstructured tetrahedral elements. For the convergence of fluid-dynamic simulations, a mesh quality check was determined using grid convergence index analysis, as assessed in a previous study of aortic hemodynamics [5]. This resulted in an element size of 0.35 mm for the aortic model. The blood flow was assumed laminar and Newtonian, with density of 1060 kg/m^3 and viscosity of 0.00371 Pa × s. Indeed, we found that the Reynolds number was 1658, and this justified the assumption of lamina flow in the large artery. Boundary flow conditions were estimated using echocardiographic data, as collected before and after aortic surgery. Specifically, the transaortic jet velocity evaluated by the Doppler ultrasound was adopted to scale the peak flow of a representative inlet flow waveform, while the time of the cardiac cycle, as determined by the heart rate, was used to scale the frequency of such representative aortic flow profiles, as done previously by our group [5,6]. The inlet flow (cardiac output of 4.7 L/min) was distributed between the supra-aortic vessels and the descending aorta with a ratio of 30/70, as done previously for the aneurysmal aorta [4,7]. For the outlet, a representative time-dependent pulsatile waveform of pressure at descending aorta

was used as a boundary condition. Figure 2 shows the profile of inlet velocity and pressure outflow used as input in the computational model.

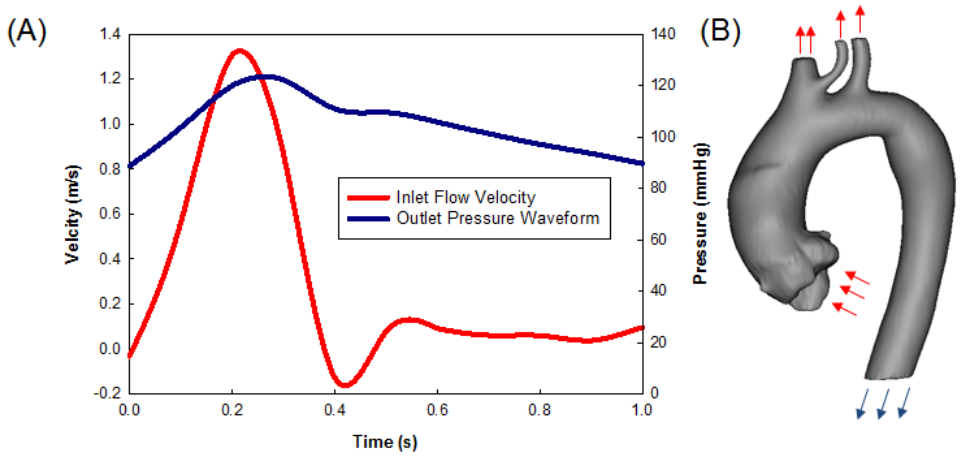

Figure 2. (**A**) Pre-operative inlet flow rate and outlet pressure waveforms and (**B**) boundary conditions prescribed in the model, with inlet velocity waveform for the aortic inlet and each of the supra-aortic arteries (as scaled versions of the aortic inlet), as well as outlet pressure waveform at the distal descending aorta.

Simulations were performed with the commercial software FLUENT v19 (Ansys Inc., Canonsburg, PA, USA). Pressure-implicit, with splitting of operators and skewness correction as pressure–velocity coupling as pressure interpolation method with 2nd order accurate discretization, was used. Convergence was enforced by reducing the residual of the continuity equation by 10−6 at every time step fixed to 0.005 s. Simulations were continued through three cardiac cycles to eliminate nonlinear start-up effects, and results were obtained at the last cycle. After the numerical solution, multiplanar data analysis of WSS and oscillatory shear index (OSI) was performed in several planes distributed uniformly along ascending aorta. Specifically, the WSS was defined:

$$\tau_w = \frac{1}{T}\int_0^T \left|\vec{t_W}\right| dt \tag{1}$$

where $\left|\vec{t_W}\right|$ is the magnitude of wall shear stress vector, $\vec{t_W}$, and T is the duration of one cardiac cycle. The OSI was defined as:

$$OSI = \frac{1}{2}\left(1 - \frac{\left|\int_0^T \vec{t_W} dt\right|}{\int_0^T \left|\vec{t_W}\right| dt}\right) \tag{2}$$

This takes values in the range of 0 to 0.5, with 0 corresponding to unidirectional flow, and 0.5 to purely oscillatory flow.

3. Results

In the preoperative model, focally elevated magnitudes of systolic WSS were observed in the anterolateral region of the ascending aorta. This resulted from the normal flow deviation secondary to the offset of the axis between the left ventricle and aortic root, as shown by Figure 3A,B. The angle between the left ventricular longitudinal axis and the aortic root (i.e., 148° before surgery and 156° after surgery) has likely influenced the jet direction and its impingement on the aortic wall from the region just above the sino-tubular junction to the mid-ascending aortic region. In a similar way, hemodynamic changes due to the presence of the bioprosthetic aortic valve replacement have occurred. After resection, we observed a redistribution of systolic WSS that spanned uniformly along the vessel circumference at the level of the mid-ascending aorta (Figure 3B). Specifically, maxima of WSS were

extrapolated from the model and then mapped onto a standardized 8-quadrant model representing 8 angular segments along the circumferential direction of the aortic wall. Thus, polar plots of WSS were obtained at three-anatomic levels: sino-tubular junction, mid-ascending aorta, distal ascending aorta (Figure 3C). Similarly, Figure 4A,B shows changes of hemodynamic parameters in 8-standardized analysis planes distributed along the longitudinal direction of the ascending thoracic aorta. An overall high mean systolic WSS was noted in the preoperative model at the level of the sino-tubular junction.

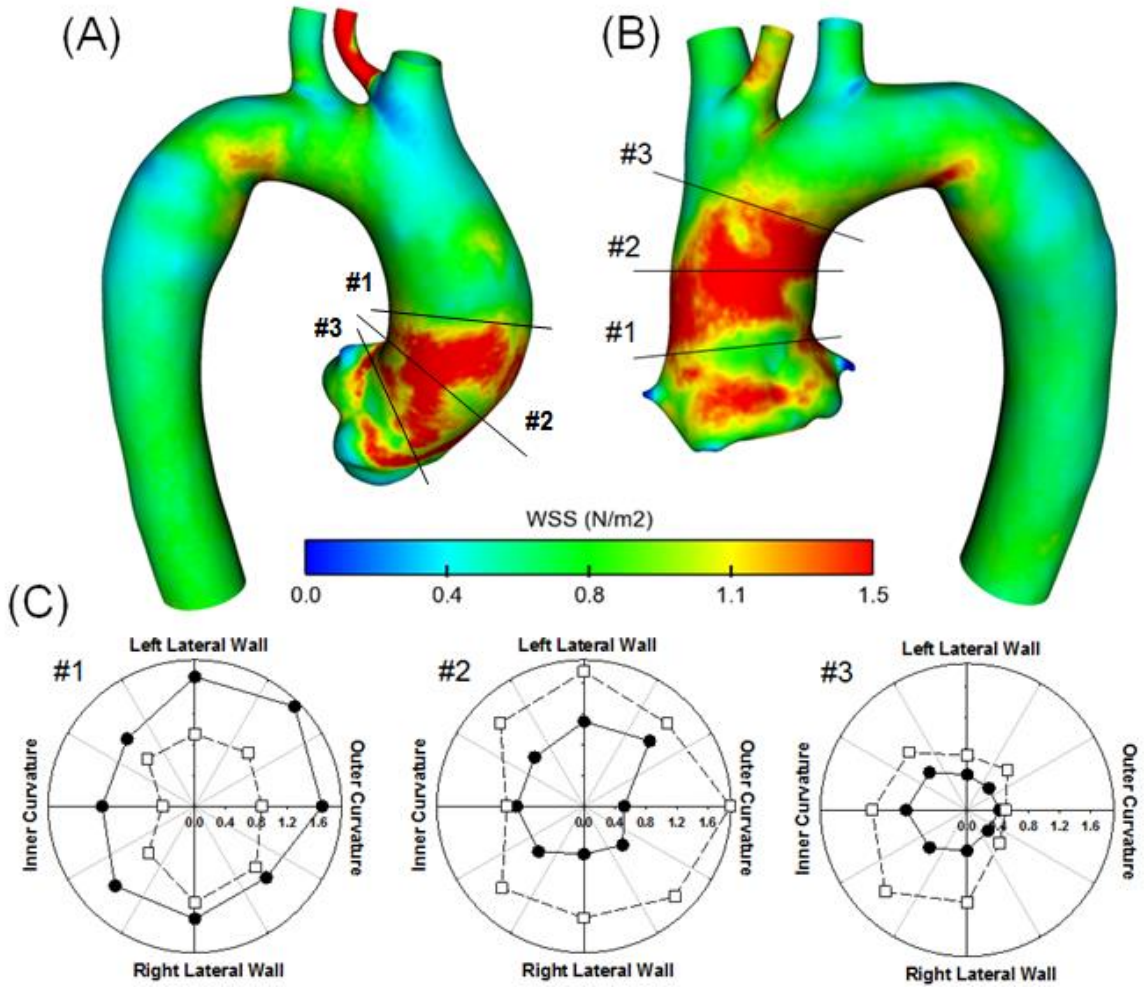

Figure 3. Map distribution of wall shear stress (WSS) at systole for (**A**) pre-operative model and (**B**) post-operative model after aortic resection; (**C**) planewise analysis of WSS using polar plots in 3 planes along ascending aorta for pre-operative (•) and post-operative (□) models.

In the post-operative model, high WSS were observed in the mid-ascending aorta and proximal aortic arch region (Figure 4A). Moreover, the preoperative scenario exhibited a progressive decrease in the values of peak systolic WSS (WSSmax) from the aortic root to the proximal arch. Differently, the profile of WSSmax of post-operative model increased markedly at distal ascending aorta. The distribution of the maximum value of OSI (OSImax), which is a marker of the directional change of WSS during the cardiac cycle, was uniformly distributed along the various levels of the aorta in the post-operative model (Figure 4B).

The fact that the post-operative model had higher WSS than the pre-operative model at proximal aortic arch is likely caused by the high systolic flow velocity (see Figure 5) observed in the ascending aorta after surgery (i.e., 1.3 m/s for pre-operative model and 1.7 m/s for post-operative model). This is likely determined by the changes in the aortic diameter and valve orifice area occurring for the remodeled aorta.

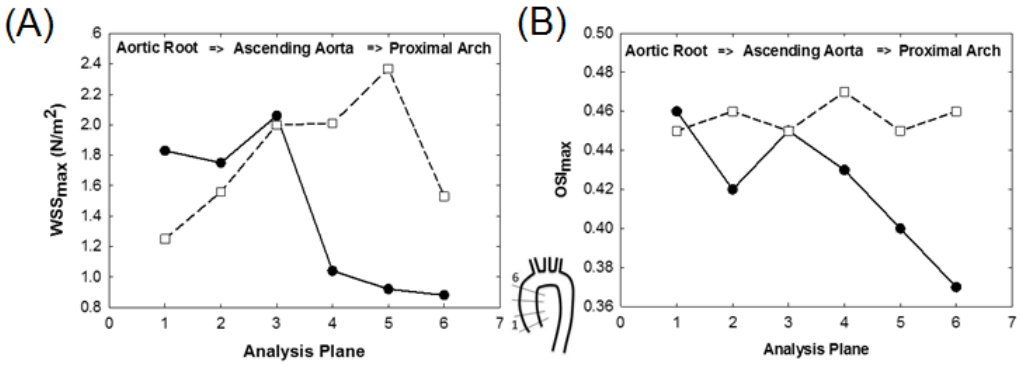

Figure 4. Distribution of (**A**) WSS_{max} and (**B**) OSI_{max} over each analysis plane within the ascending aorta for pre-operative (•) and post-operative (□) models, as indicated by the scheme in the center.

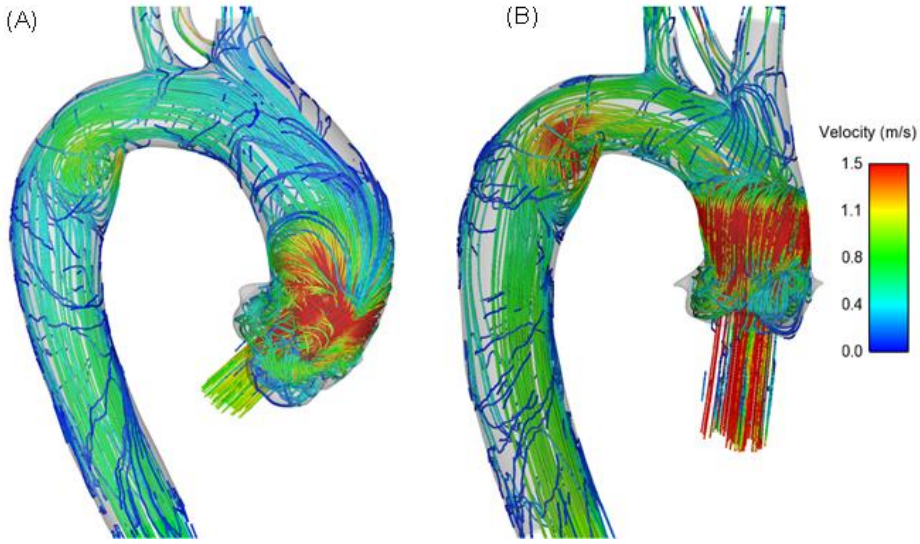

Figure 5. Flow streamlines at peak systole, as obtained from the computational modeling of (**A**) pre-operative model and (**B**) post-operative model.

4. Discussion

Current guidelines put the cut-off for ascending aorta replacement at 5.5 cm, but aortic rupture, dissection, and death have been reported in over 5% of patients, with aortic dimensions between 4.0 and 4.9 cm [7]. Although aortic resection and end-to-end anastomosis have been proposed to treat ascending aortic aneurysms [1,8], this has never been suggested as a preventive method to manage aortic ectasia in patients undergoing surgical treatment for other cardiac conditions. Additionally, the complex relationships between hemodynamic stress and genetic factors leave open the debate on the strategies of prevention and timing, as well as the optimal surgical technique. The criteria for the extent of resection are also currently subject to wide variations according to the individual surgeon or center experience. There are also not any long-term studies on the risk of reoperation of repaired aneurysmal ascending aorta. However, considering the significant proportion of patients developing aortic dilatation, a low percentage of reoperations on the residual aorta (about 1% in the Mayo series over a median 3-year follow-up [9]) may represent a large health care burden.

In this way, computational modeling offers a patient-specific analysis of the hemodynamic environment pre- and after surgery of the aneurysmal aorta. Computational modeling may help identify quantitative changes in hemodynamic parameters after surgical correction [10]. If adopted pre-operative, modeling results can help to guide surgeons in optimizing the extent of aortic surgery and identify patients at high-risk of post-operative complications. The most striking finding of this

patient case study is that shear stress after resection of aortic ectasia redistributes uniformly along the vessel circumference and length, as a result of the remodeled ascending aortic anatomy. Although these results cannot be used to formulate a general rule to exclude the risk of post-operative flow-related complications induced by the remodeled aorta, the result emphasizes the need for patient-specific analysis of the aorta, as well as the analysis on large patient cohort for a detailed assessment of the implication of WSS on aortoplasty. This can ultimately improve the rationale of the surgical procedure, by developing patient-tailored approaches.

Indeed, WSS are reduced near the aortic root and redistribute along the vessel circumference at the distal aortic portion. Since WSS is the velocity gradient near the aortic wall, the high flow velocity of post-operative model has likely increased the values of WSS at proximal aortic arch when compared to those of the pre-operative scenario. Therefore, we cannot assess that the distribution of WSS near the distal ascending aorta does not portend further aneurysmal redilatation after aortic remodeling. Differently, the low shear stress values near the aortic root suggest a reduced risk of post-operative complications. This is supported by the fact that, when this simplified procedure is performed to treat ascending aortic aneurysms without interposition of a prosthetic graft, ascending aorta re-dilatation and/or dissection will not occur, even at long-term follow-up [1]. In the reported case, the aortic remodeling induced high WSSmax and OSImax near the mid-ascending aorta and proximal aortic arch, since the flow jet impinges the aortic wall more distally than that of the pre-operative aorta. While it has been demonstrated that the mechanical damage of endothelial layer is associated to changes in WSS, the extent to which that response plays a role in the aneurysm formation and progression has yet to be demonstrated.

Our study has a series of limitations. The main assumption is related to the boundary conditions set at both inlet and outlet boundaries of the aorta. Estimations of WSS and OSI parameters could benefit from a magnetic resonance imaging study to determine patient-specific time-varying flow conditions, which can be then implemented in the computational model. Blood viscosity and wall compliance were not considered, but the effect of these parameters were shown by our group to have a limited impact on WSS predictions [10]. Specifically, the blood is a non-Newtonian fluid, so that the change in the blood viscosity with shear stress may have altered the prediction of the aortic hemodynamic. However, Khanafer and collaborators [11] showed that the non-Newtonian assumption of blood affects the blood flow in the thoracic aorta; their simulations did not display significant differences in WSS calculated from Newtonian and non-Newtonian fluids. In future studies, non-Newtonian fluids will be implemented to improve the prediction of the proposed computational flow analysis. Moreover, the flow analysis has been performed only on one patient's dataset thus far, and hence the results are preliminary and warrant, to be clinically relevant, a validation study on a larger number of datasets.

5. Conclusions

We conclude that an end-to-end anastomosis of ascending aorta ectasia may favorably modify aortic hemodynamic. Further studies should be performed to elucidate the long-term benefits in terms of hemodynamics and the reduction of aortic complications in patients operated on for concomitant cardiac conditions.

Author Contributions: Conceptualization, G.M.R. and S.P.; methodology, S.P.; software, S.P.; validation, G.M.R. and S.P.; investigation, S.P.; resources, S.P.; data curation, G.M.R. and S.P.; writing—original draft preparation, G.M.R. and S.P; writing—review and editing, G.M.R. and S.P.; supervision, G.M.R. and S.P.; funding acquisition, S.P. All authors have read and agreed to the published version of the manuscript.

Funding: This research was funded by Ministero della Salute, grant number GR-2011-02348129.

Conflicts of Interest: The authors declare no conflict of interest. The funders had no role in the design of the study; in the collection, analyses, or interpretation of data; in the writing of the manuscript, or in the decision to publish the results.

References

1. Massetti, M.; Veron, S.; Neri, E.; Coffin, O.; le Page, O.; Babatasi, G.; Buklas, D.; Maiza, D.; Gerard, J.L.; Khayat, A. Long-term durability of resection and end-to-end anastomosis for ascending aortic aneurysms. *J. Thorac. Cardiovasc. Surg.* **2004**, *127*, 1381–1387. [CrossRef] [PubMed]
2. Lee, J.J.; D'Ancona, G.; Amaducci, A.; Follis, F.; Pilato, M.; Pasta, S. Role of computational modeling in thoracic aortic pathology: A review. *J. Card. Surg.* **2014**, *29*, 653–662. [CrossRef] [PubMed]
3. Cosentino, F.; Scardulla, F.; D'Acquisto, L.; Agnese, V.; Gentile, G.; Raffa, G.; Bellavia, D.; Pilato, M.; Pasta, S. Computational Modeling of Bicuspid Aortopathy: Towards Personalized Risk Strategies. *J. Mol. Cell. Cardiol.* **2019**, *4*, 122–131. [CrossRef] [PubMed]
4. Rinaudo, A.; Raffa, G.M.; Scardulla, F.; Pilato, M.; Scardulla, C.; Pasta, S. Biomechanical implications of excessive endograft protrusion into the aortic arch after thoracic endovascular repair. *Comput. Biol. Med.* **2015**, *66*, 235–241. [CrossRef] [PubMed]
5. Gallo, A.; Agnese, V.; Coronello, C.; Raffa, G.M.; Bellavia, D.; Conaldi, P.; Pilato, M.; Pasta, S. On the Prospect of Serum Exosomal miRNA Profiling and Protein Biomarkers for the Diagnosis of Ascending Aortic Dilatation in Patients with Bicuspid and Tricuspid aortic Valve. *Int. J. Cardiol.* **2018**. [CrossRef] [PubMed]
6. Pasta, S.; Agnese, V.; Di Giuseppe, M.; Gentile, G.; Raffa, G.M.; Bellavia, D.; Pilato, M. In-vivo Strain Analysis of Dilated Ascending Thoracic Aorta by ECG-gated CT Angiographic Imaging. *Ann. Biomed. Eng.* **2017**, *45*, 2911–2920. [CrossRef] [PubMed]
7. Davies, R.R.; Goldstein, L.J.; Coady, M.A.; Tittle, S.L.; Rizzo, J.A.; Kopf, G.S.; Elefteriades, J.A. Yearly rupture or dissection rates for thoracic aortic aneurysms: Simple prediction based on size. *Ann. Thorac. Surg.* **2002**, *73*, 17–28. [CrossRef]
8. Ikonomidis, J.S.; DeAnda, A.; Miller, D.C. Resection of ascending aortic aneurysm without use of an interposition aortic graft. *J. Thorac. Cardiovasc. Surg.* **2001**, *122*, 395–397. [CrossRef] [PubMed]
9. Park, C.B.; Greason, K.L.; Suri, R.M.; Michelena, H.I.; Schaff, H.V.; Sundt, T.M., 3rd. Fate of nonreplaced sinuses of Valsalva in bicuspid aortic valve disease. *J. Thorac. Cardiovasc. Surg.* **2011**, *142*, 278–284. [CrossRef] [PubMed]
10. Mendez, V.; Di Giuseppe, M.; Pasta, S. Comparison of Hemodynamic and Structural Indices of Ascending Thoracic Aortic Aneurysm as predicted by 2-way FSI, CFD Rigid Wall Simulation and Patient-Specific Displacement-Based FEA. *Comput. Biol. Med.* **2018**. [CrossRef] [PubMed]
11. Khanafer, K.; Berguer, R. Fluid-structure interaction analysis of turbulent pulsatile flow within a layered aortic wall as related to aortic dissection. *J. Biomech.* **2009**, *42*, 2642–2648. [CrossRef] [PubMed]